

Pore Size Distribution and Porosities of Nano-TiO_2 Films Made by Using Cellulosic Thickener and Their Influence on Performance of Dye-Sensitized Solar Cells

Ke-Jian Jiang, Takayuki Kitamura, Yuji Wada, and Shozo Yanagida*

Material and Life Science, Graduate School of Engineering, Osaka University,
2-1 Yamada-oka, Suita, Osaka 565-0871

Received March 31, 2003; E-mail: yanagida@mls.eng.osaka-u.ac.jp

A series of mesoporous TiO_2 films with different average pore sizes and distributions were prepared by changing the addition content of cellulosic thickener in the pastes. The BET surface area shows that, for the samples with 3, 5, 10 and 15 wt % cellulosic thickener, the average pore size remained centered at 14–15 nm, but the pore size distribution became narrower with the increase of cellulosic thickener addition. With further increase of cellulosic thickener to 21 and 30 wt %, the average pore size decreases to 13 and 11 nm, and the pore size distribution also became much narrower. The sample, prepared from the paste with 15 wt % cellulosic thickener, shows the best result: short-circuit photocurrent density 13 mA/cm^2, open-circuit photovoltage 0.72 V, fill factor 0.68, and conversion efficiency 6.4%.

Dye-sensitized solar cell (DSC) is one of the most promising candidates for the conventional solar cell owing to its high efficiency, simple fabrication and low production cost.[1–11] High conversion efficiency of up to 10%, being comparable with amorphous silicon solar cells, has been reported by the Grätzel group.[2] Recently, many researchers mainly focused on finding new dyes to improve the light-harvesting of DSCs, on developing new electron-transfer mediators to replace volatile and corrosive iodide/triiodide redox system, and on studying the mechanism of DSCs. However, fewer studies were done about pore size and its distribution of the semiconductor electrodes, and their influences on the photoelectric performance of DSCs.

Barbé et al. studied the influence of binder addition on the pore size, pore-size distribution and photovoltaic properties.[3] Their results showed that, for the proportion of 0–30 wt % polyethylene glycol (PEG) binder of the TiO_2 in pastes, the average pore size of sintered mesoporous TiO_2 films remained centered at 30 nm, while the distribution became broader toward the larger pores with increasing PEG content. With PEG increasing up to 50 wt %, the average pore size increased to 50 nm, and pore size distribution became much broader, with pores as large as 120 nm. The report also showed that the short-circuit current and conversion efficiency decreased gradually with increase of PEG addition. Srikanth et al. also reported the influence of the PEG addition concentration in the sol–gel TiO_2 pastes for spin coating on the surface morphology and solar cell performances.[10] The results showed that conversion efficiencies increased with PEG addition up to 40 wt % of TiO_2, and decreased with further addition. These two papers clearly reported the relation between the preparation conditions of the paste and the morphology of the resulting mesoporous films, but only short discussions were presented for the relation between the morphology of the film and the solar cell performances.

We previously reported that Showa-Titanium (F-6), which was prepared in vapor phase hydrolysis from $TiCl_4$ and O_2, was found to form nice mesoporous TiO_2 films when cellulosic thickener was employed as additives for the paste suitable for screen printing. The cells based on the F-6 films showed high photoelectric performance comparable to the cell with P25 TiO_2 film, which is often used as the standard.[6] In this paper, we report the pore size, pore distribution and porosity in the TiO_2 films prepared by changing the cellulosic thickener concentration in the pastes, and present the relationship between the amount of the adsorbed dye on the film and pore size and porosity of the resulting TiO_2 films. The performances of the dye-sensitized solar cells based on the different TiO_2 films were investigated by means of the morphology. The differences of the morphological changes of the TiO_2 films prepared from the paste with PEG and cellulosic thickener were also discussed.

Experimental

Commercial TiO_2 nanoparticles (F-6, a mixture of ca. 5% rutile and 95% anataste, average diameter 16 nm, BET surface area 96 m^2/g) were supplied from Showa Titanium, in Japan. Cellulosic thickener (60MP-50), with viscosity of 100 cps in the 2.5 wt % aq. solution, was supplied from Matsumoto Yushi-seiyaku in Japan. The TGA analysis was run on a thermogravimeter analyzer (Shimadzu, TGA-50). The sample was heated from room temperature to 500 °C at 5 °C/min under aerated conditions.

The TiO_2 powder and zirconium oxide beads (diameter: 3 mm) were put in a plastic bottle with some amount of water containing cellulosic thickener of different weight ratio to TiO_2 in the paste, and dispersed by using a paint shaker (Red Devil Equipment, 5410). Table 1 shows the composition of different pastes. In order to acquire smooth films, some pentanol were added to the pastes to remove the bubbles caused during preparation of pastes and films. The TiO_2 paste was applied to a conducting glass sheet (coated with F-doped SnO_2, 10–12 Ω/□, Nippon Sheet Glass). The TiO_2 film thickness was controlled to be about 10 μm with three layers

Published on the web December 15, 2003; DOI 10.1246/bcsj.76.2415

Table 1. Composition of TiO_2 Paste with Different Weight Ratio of Cellulosic Thickener

Sample No.	TiO_2 /g	Cellulosic thickener/g	Pentanol /g	H_2O /g
1	7	0.21	5	14.7
2	7	0.35	5	22
3	7	0.7	5	28
4	7	1.05	5	38
5	7	1.5	5	70
6	7	2.1	5	75

of Scotch Tape adhered to the glass as a spacer. After air drying, the electrodes were sintered for 30 min at 500 °C. The resulting film thickness was measured with a profiler (Sloan, Dektak3). The TiO_2 electrodes were immersed overnight in a 0.3 mM (1 M = 1 mol/dm^3) ethanolic solution of ruthenium dye (*cis*-dithiocyanate-*N*,*N*′-bis(4-carboxylate-4-tetrabutylammoniumcarboxylate-2,2′-bipyridine)ruthenium(II); N719). The resulting dye absorbed electrode was assembled with a Pt-sputtered conducting glass to form a sandwich-type dye cell. The electrolyte solution was composed of 0.1 M LiI, 0.3 M 1,2-dimethyl-3-propylimidazolium iodide, 0.05 M I_2 and 0.5 M 4-*tert*-butylpyridine in methoxyacetonitrile. The detailed description for the photocurrent-voltage measurement was given elsewhere.[5] The amount of dye adsorbed on the film was determined by desorbing the dye from the TiO_2 surface into an aqueous solution of 0.01 M NaOH and measuring its absorption spectrum.

The BET surface area of the TiO_2 film, coated with pastes containing different concentrations of cellulosic thickener, was recorded by a nitrogen adsorption–desorption apparatus (Quantachrome, Autosorb-1), and pore diameters and volume were also determined using the BJH method of nitrogen desorption measurements.

Results and Discussion

It should be noted that it is difficult to form a nice TiO_2 film without cellulosic thickener additive in the TiO_2 (F-6) paste. Figure 1 shows the influence of cellulosic thickener addition on the pore size distribution of TiO_2 films. It is clear that only 3 wt % cellulosic thickener decreased the average pore size from 24 nm to 14 nm, which suggests that cellulosic thickener improved the binding of TiO_2 nanoparticles, and then decreased the pore size among the particles. One can see from Fig. 1 that, for the samples with 3, 5, 10, 15 and 21 wt % of cellulosic thickener, the average pore size remained centered at 14–15 nm, but the pore size distribution became narrower with the increase of cellulosic thickener addition, opposite to the case reported using PEG as an additive. With further increase of cellulosic thickener from 21 to 30 wt %, average pore size decreased from 13 to 11 nm, and the pore size distribution also became much narrower, which is different from the case of PEG. Barbé et al. reported the influence of PEG binder additive on the pore size. Their results show that, for 0–30 wt % PEG binder in pastes, the average pore size didn't change; on further increasing PEG to 50 wt %, the pore size distribution became broader, and average pore size increased from 30 to 50 nm.[3] We previously reported the relationship of the TiO_2 morphology and solar cell performances, in which PEG was used as the binder and the size of pores of the mesoporous film was precisely controlled.[12] PEG adhere to the surface of TiO_2 particles through hydrogen bonds, but also take a helical structure in the bulk.[13] While under low concentration conditions TiO_2 particles in the paste were surrounded by adsorbed PEG molecules through hydrogen bonds, under high concentration conditions, an excess amount of PEG seems to exist as large aggregates with helical structure, which behave like particles in the paste and burn out during calcination and sintering. Therefore, the larger amount of PEG can generate large-sized pores in the TiO_2 film after sintering at high temperature. In contrast to PEG, the pore sizes decrease with increase of cellulosic thickener from 3 to 30 wt %, which might be ascribed to chemical structure of cellulosic thickener, which is different from that of PEG. The thickener is soluble in water, because hydroxy groups of cellulose are randomly substituted to prevent the formation of tight aggregates through the intermolecular hydrogen bond formation in aqueous solution.[6] It would have moderate hydrophilicity, enough to adsorb on the surface of TiO_2 particles but not enough to form aggregates in the paste. Thus the hydrophilic (hydroxy and ether) groups in cellulosic thickener can help to bind hydrophilic TiO_2 nanoparticles through hydrogen bonds in the TiO_2 paste, and the pore size of the sintered film will decrease with increase of cellulosic thickener content.

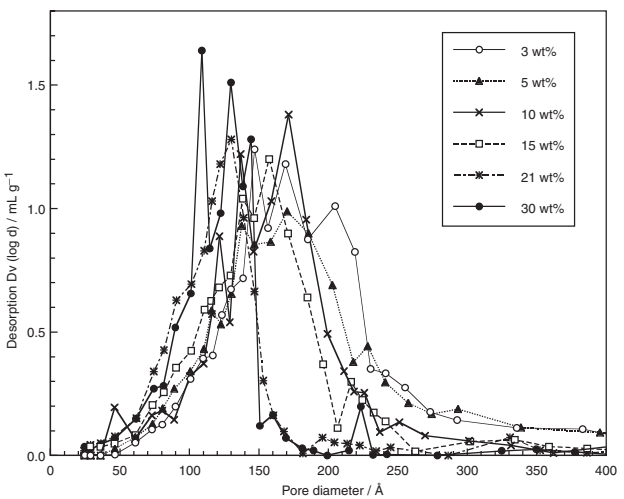

Fig. 1. Influences of the weight ratio of cellulosic thickener to TiO_2 [(○) 3, (▲) 5, (×) 10, (□) 15, (∗) 21, (●) 30 wt %] in the paste on pore size distribution of the sintered films.

Figure 2 shows TGA curve of cellulosic thickener used in the TiO_2 pastes as the additive. TGA curve from room temperature

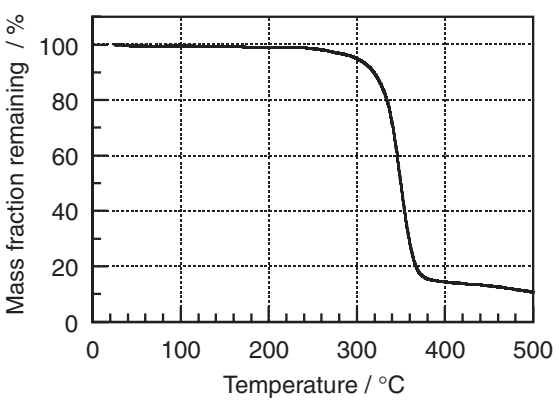

Fig. 2. TGA analysis of cellulosic thickener in air.

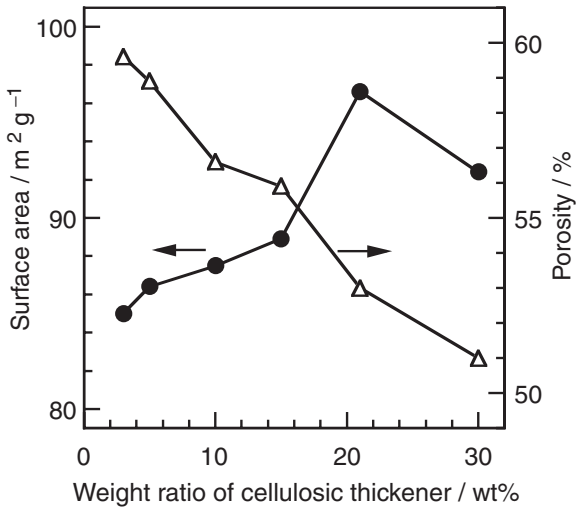

Fig. 3. Influence of the weight ratio of cellulosic thickener to TiO_2 in the paste on surface area and porosity of the sintered films.

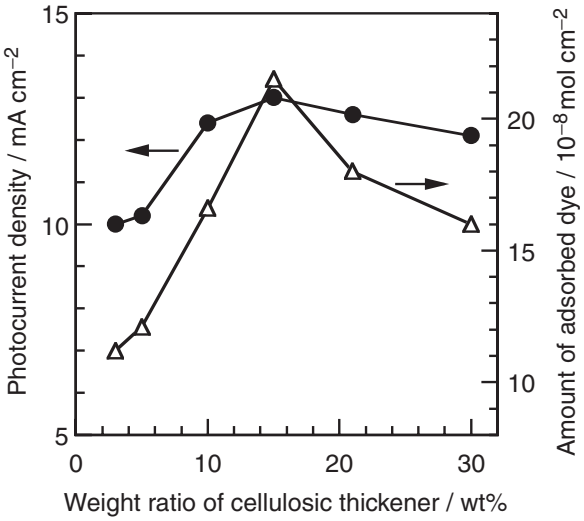

Fig. 4. Influence of the weight ratio of cellulosic thickener to TiO_2 in the paste on dye adsorption to the sintered films and photocurrent density of the dye-sensitized solar cell based on the film.

to ca. 250 °C represented vaporization of the volatile materials such as residual absorbed water, from 250 to 400 °C represented the main thermal degradation of the thickener through vaporization, combustion and carbonization, and from 400 °C showed the further burning of the carbonized thickener.

Figure 3 shows an influence of the weight ratio of cellulosic thickener on surface area and porosity in TiO_2 films after sintering. It can be found that porosity decreased gradually from 60% to 51% with the increase of cellulosic thickener addition from 3 to 30 wt %. Therefore, one can speculate that the cellulosic thickener assists the binding between TiO_2 nanoparticles and decreases the pore size during sintering. For the samples with 3, 5, 10 and 15 wt % cellulosic thickener, the surface area of TiO_2 films remained between 85–89 m^2/g while the average pore size was about 14–15 nm (in Fig. 1). The observation can be explained as due to effective thermal necking between TiO_2 particles without size growth. With further increase to 21 wt %, the surface area increased to 97 m^2/g and the average pore size decreased to ca. 13 nm. When the cellulosic thickener increased to 30 wt %, some TiO_2 nanoparticles might undergo effective necking growth, giving smaller average pore size (ca. 11 nm), followed by the slight decrease in the surface area from 97 to 92 m^2/g. As discussed above, free PEG thickener could exist as aggregates in the paste, contributing to the formation of larger pores after sintering.[12] Thus the increase of PEG addition increases the pore diameter and porosity, and then widens the pore size distribution. In the case of cellulosic thickener, however, the thickener addition enhanced mainly neck growth between the particles and the thickener could not form bulky aggregates in the paste. Further addition of the thickener induces only necking of the particles during sintering, resulting in a decrease of the pore diameter.

Figure 4 shows the influence of cellulosic thickener on the amount of adsorbed dye and photocurrent density. From Fig. 4, we can find that the amount of adsorbed dye increased sharply from 1.1×10^{-7} to 2.2×10^{-7} mol/cm^2 with the increase of cellulosic thickener from 3 to 15 wt %, but further increase of cellulosic thickener caused a slight decrease of the dye amount from 2.2×10^{-7} to 1.6×10^{-7} mol/cm^2. However, the change of dye adsorption was not proportional to the change of surface area. This would be explained as due to the effective formation of dye-adsorption sites on TiO_2 particles. In other words, the amount of dye adsorption would depend not only on the surface area but also on the specific adsorption sites of the particles, because N719 dye has a rigid structure and adsorbs on TiO_2 surface through two carboxylic groups.[14] Some amorphous phase on the surface and crystalline surface such as step or kink might change into more favorable surface structure for dye adsorption during the sintering, in particular, in the presence of effectual amounts of the thickener (<15 wt %).[15] Neck growth between TiO_2 particles was enhanced in the presence of cellulosic thickener, but excess of the thickener might induce the close aggregation reducing the effective adsorption sites on TiO_2 particles.

From Fig. 4, we also can find that photocurrent density increased from 10 to 13 mA/cm^2 with the increase of the amount of adsorbed dye from 1.1×10^{-7} to 2.2×10^{-7} mol/cm^2, which is ascribed to the effective increase of light absorption of the increased dye molecules. The photocurrent density of dye-sensitized solar cells is proportional to the number of absorbed photons that is determined primarily by the amount of dye on the TiO_2 electrode. The number of photons, however, will be saturated at shorter wavelength region ($\lambda < 550$ nm) when the amount of dye adsorption is too high, and only the increment of absorptivity at longer wavelength region will contribute to the further increase of photocurrent, because N719 dye has a high absorption coefficient at this region. Thus the photocurrent density deviates from the linear relation with the amount of dye adsorption. This is also true for the plot of the photocurrent density vs thickness of TiO_2 film.[5]

Table 2 shows the performance of dye-sensitized solar cells based on different TiO_2 films. Among samples from No. 1 to 6, No. 4, which was prepared from the paste containing 15 wt % cellulosic thickener, shows the best result: short-circuit photocurrent density 13 mA/cm^2, open-circuit photovoltage 0.72 V,

Table 2. Performance of Dye-Sensitized Solar Cells Based on Different TiO_2 Films

Sample No.	J_{sc}/mA cm^{-2}	V_{oc}/V	*FF*	*Eff*/%
1	10.0	0.69	0.61	4.24
2	10.2	0.71	0.65	4.55
3	12.4	0.73	0.71	6.36
4	13.0	0.72	0.68	6.40
5	12.6	0.69	0.68	6.00
6	12.1	0.72	0.69	6.00

fill factor 0.68, and conversion efficiency 6.4%. The resulting values are reliable and comparable to those found in the previous works.

Conclusions

1. The cellulosic thickener starts to burn around 300 °C. From 300 to 400 °C, the exclusive thermal combustion of the cellulosic thickener occurs, leading to calcination and carbonization; at higher than 400 °C, the carbonized cellulosic thickener is further combusted gradually.

2. For the samples with 3, 5, 10 and 15 wt % cellulosic thickener, the average pore size remained centered at 14–15 nm, but the pore size distribution became narrower with the increase of cellulosic thickener addition. On further increase of the thickener to 21 and 30 wt %, the average pore size decreased to 13 and 11 nm, respectively, and the pore size distribution also became much narrower.

3. Photocurrent density increased from 10 to 13 mA/cm^2 with the amount of adsorbed dye increased from 1.1×10^{-7} to 2.2×10^{-7} mol/cm^2. This is ascribed to the fraction of light adsorbed by dye, expected to determine the current density. Sample No. 4, with 15 wt % cellulosic thickener, showed the best result: short-circuit current density 13 mA/cm^2, open-circuit voltage 0.72 V, fill factor 0.68, and conversion efficiency 6.4%.

This work was partially supported by a Grant-in-Aid for the Scientific Research (Grant 11358006) and by a Grant-in-Aid for the Creation of Innovations through Business-Academic-Public Sector Cooperation, Open Competition for the Development of Innovative Technology (No. 12310) from the Ministry of Education, Culture, Sports, Science and Technology. KJJ also acknowledges to the Research Institute of Innovative Technology for the Earth (RITE), Japan.

References

1 B. O'Regan and M. Grätzel, *Nature*, **353**, 737 (1991).

2 M. K. Nazeeruddin, A. Kay, I. R. Humphry-Baker, E. Müller, P. Liska, N. Vlachopoulos, and M. Grätzel, *J. Am. Chem. Soc.*, **115**, 6382 (1993).

3 C. J. Barbé, F. Arendse, P. Come, M. Jirousek, F. Lenzmann, V. S. Shklover, and M. Grätzel, *J. Am. Ceram. Soc.*, **80**, 3157 (1997).

4 K. Murakoshi, R. Kogure, Y. Wada, and S. Yanagida, *Sol. Energy Mater. Sol. Cells*, **55**, 113 (1998).

5 S. Kambe, K. Murakoshi, T. Kitamura, Y. Wada, S. Yanagida, H. Kominami, and Y. Kera, *Sol. Energy Mater. Sol. Cells*, **61**, 427 (2001).

6 D.-S. Zhang, S. Ito, Y. Wada, T. Kitamura, and S. Yanagida, *Chem. Lett.*, **2001**, 1042.

7 N.-G. Park, G. Schlichthorl, J. van de Lagemaat, H. M. Cheong, A. Mascarenhas, and A. J. Frank, *J. Phys. Chem. B*, **103**, 3308 (1999).

8 N.-G. Park, J. van de Lagemaat, and A. J. Frank, *J. Phys. Chem. B*, **104**, 8989 (2000).

9 J. Weidmann, Th. Dittrich, E. Konstantinova, I. Lauermann, I. Uhlendorf, and F. Koch, *Sol. Energy Mater. Sol. Cells*, **56**, 153 (1999).

10 K. Srikanth, Md. M. Rahman, H. Tanaka, K. M. Krishna, T. Soga, M. K. Mishra, T. Jimbo, and M. Umeno, *Sol. Energy Mater. Sol. Cells*, **65**, 171 (2001).

11 S. Lee, Y. Jun, K. J. Kim, and D. Kim, *Sol. Energy Mater. Sol. Cells*, **65**, 193 (2001).

12 S. Saito, S. Kambe, T. Kitamura, Y. Wada, and S. Yanagida, *Sol. Energy Mater. Sol. Cells*, in press.

13 Y. Takahashi and H. Tadokoro, *Macromolecules*, **6**, 672 (1973).

14 V. Shklover, Y. E. Ovchinnikov, L. S. Braginsky, S. M. Zakeeruddin, and M. Grätzel, *Chem. Mater.*, **10**, 2533 (1998).

15 S. Nakade, M. Matsuda, S. Kambe, Y. Saito, T. Kitamura, T. Sakata, Y. Wada, H. Mori, and S. Yanagida, *J. Phys. Chem. B*, **106**, 10004 (2002).